Formation Control of Leader-Following UAVs to Track a Moving Target in a Dynamic Environment

AnhDuc Dang and Joachim Horn
Helmut Schmidt University / University of the Federal Armed Forces Hamburg, Institute of Control Engineering, D-22043 Hamburg, Germany
Email: {adang, Joachim.horn}@hsu-hh.de

***Abstract*—This paper presents a new approach to formation control of a swarm of unmanned aerial vehicles (UAVs) to track a moving target in dynamic environment based on the artificial potential field method combined with a state feedback controller. In this approach, an attractive potential field is generated between the leader and the target by the relative position of them to drive the leader to track the target. The other robots in the swarm are controlled by the attractive potential field between them and the leader to follow the leader. By the influence of the potential field between neighboring robots, the organization of the swarm is stable and robust, and the collisions do not happen in the swarm. Obstacle avoidance is driven by a repulsive potential field thatis created in the region around the obstacles. The effectiveness of the proposed approach has been verified in simulations.**

***Index Terms*—formation control, potential field method, nonlinear control, aircraft control**

I. Introduction

Formation control of multi-robot systems has been one of the interesting research topics in the control community all over the world in recent years. Its potential applications in many areas such as search and rescue missions, forest fire detection and surveillance is the motivation and reason for this attraction.

In the formation control of multi-robot systems, the moving trajectory determination of each member-robot and the control of the motion of it along this determined trajectory are crucial problems. One of the effective and interesting methods to solve these problems is the artificial potential field method presented in [1]-[3]. In this method, the motion of the robots is controlled by artificial force fields considering the relative positions of the robots, target and obstacles of the environment.

In recent years, the artificial potential field method has been widely studied and used to control a group of mobile robots to reach the position of the target with the environmental influence in 2D (two-dimensional) space, see [4]-[7]. Using this control method the stability and robustness of the group are attained. Furthermore, this method has been developed und applied to the path planning of flight robots in 3D (three-dimensional) space when the target and obstacles are stationary [11], [12].

In this paper, the artificial potential field method is extended and applied to formation control of a swarm of UAVs, which follows the robot-leader to track a moving target through the obstacles of the environment. One UAV in the swarm is appointed as the leader. By the attraction of the artificial potential field from the target, the leader will drive its swarm to approach the target position. Each member-robot will be connected with its neighbors by the artificial potential field, which consists of an attractive and a repulsive potential field among them. The moving trajectory of each member-robot is controlled by the total potential field consisting of the attractive field of the leader, the repulsive field around the obstacles, and the attractive/repulsive fields of its neighbors. The state feedback controller, which is built by the Backstepping method see [10], will regulate the robot to reach this desired trajectory. Using this total force field, with the leader tracking a moving target, the robustness and stability of the swarm are maintained on a desired altitude that is chosen by the altitude of the target. Obstacle and collision-avoidance of the swarm are solved effectively.

This paper is organized as follows: The problem statement is given in the next section. Section III presents the control algorithm for the swarm using the potential field method. In section IV, the stability and robustness analysis of the swarm based on the Lyapunov theory is given. Section V presents the mathematical model of the UAV and the nonlinear controller using the Backstepping method. Some simulation results are presented in section VI. And finally, section VII concludes this paper and proposes future research works.

II. Problem Statemant

In this section we will consider that a swarm of N UAVs flies in a three-dimensional Euclidean space with Mobstacles.

Each robot's motion, which can be viewed as a moving point in the space, is described by the dynamic model as:

Manuscript received July 16, 2013; revised February 11, 2014.

doi: 10.12720/joace.3.1.1-8

$$\begin{cases} \dot{p}_i = v_i \\ \dot{v}_i = \dfrac{1}{m} u_i \end{cases} \quad i = 1, \ldots N. \tag{1}$$

Here $(p_i, v_i) \in R^3$ *and* m are the position vector, the velocity vector and the mass of the robot i in 3D respectively. The control input u_i of the robot i is designed by the artificial potential field method (see [1], [3]) based on the relative positions between the robot i with its neighbors, the leader and the obstacles in the environment combined with the relative velocities among them.

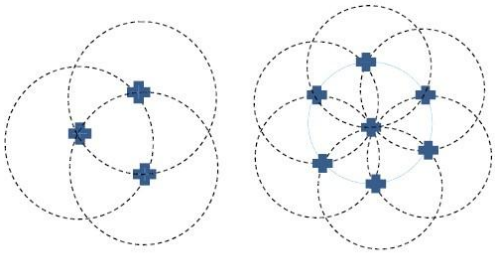

a) b)

Figure 1. Configuration of a desired swarm of three (a) and seven robots (b).

The idea for the stability and robustness of a desired swarm of UAVs (example in Fig. 1) is shown about the constant distance between each robot i and its neighbors. Let $N_i^{\alpha}(t)$ be the set of the α neighborhood of the robot i at time *t*. One robot *j*, which is the neighbor of the robot i ($j \in N_i^{\alpha}(t)$), is defined as follows:

$$\left\{ j \in N_i^{\alpha}(t) \right\} = \left\{ j, d_i^j \le r^{\alpha}, j = 1, \ldots N, j \ne i, j \ne l \right\} \tag{2}$$

where $r^{\alpha} > 0$ is an interaction range (radius of neighborhood circle, show in Fig. 4) and $d_i^j = \left\| q_i - q_j \right\|$ is the Euclidean distance. In many cases, the relative distance between the robots can be changed while avoiding obstacles or changing moving direction, therefore the neighbors of each robot *i* can also be changed, and then the new stable structure of the swarm will continue to perform.

III. Formation Control

This section presents the algorithm for the formation control of the leader-following UAVs to track a moving target while avoiding obstacles in the environment based on the artificial potential field method.

A. Control Algorithm for the Robot-Leader

The motion of the robot-leader is driven by the total artificial force that consists of two components as follows:

$$u_l = f_l^t + f_l^o. \tag{3}$$

The first component f_l^t is an attractive force to control the robot-leader to reach a moving target. It is represented asin [1]-[6]:

$$V_{att} = \frac{1}{2} k_l^t \left(p_l - p_t \right)^T \left(p_l - p_t \right) \tag{4}$$

$$f_l^t = -\nabla V_{att} = -k_l^t \left(p_l - p_t \right) \tag{5}$$

where the negative gradient of the potential function V_{att} is ($-\nabla V_{att}$)and $\left(p_l - p_t \right)$ is the relative position of the target and the robot-leader.

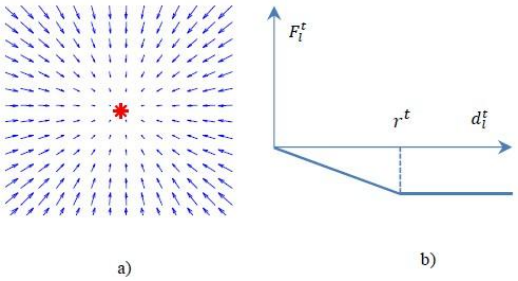

a) b)

Figure 2. The sketch of vector field $F_l^t n_l^t$ directed toward the target position (a) and value of the force F_l^t depending on distance d_l^t (b) .

In our approach, the relative velocity among the leader and the target is added in the attractive force which is used as a damping term to control the robot-leader when it approaches the target position.This attractive force is proposed as follows:

$$f_l^t = F_l^t n_l^t - k_l^{vt} \left(v_l - v_t \right) \tag{6}$$

where $n_l^t = \dfrac{\left(p_l - p_t \right)}{\left\| p_l - p_t \right\|}$ is a unit vector along the line connection p_l to p_t and $\left(v_l - v_t \right)$ is the relative velocity between them used as a damping term with the positive amplification coefficient k_l^{vt} . The attractive force field $F_l^t n_l^t$ depicted in Fig. 2 is calculated as follows:

$$F_l^t n_l^t = -\nabla V_l^t \tag{7}$$

where the potential function V_l^t of this vector field is built as:

$$V_l^t = \begin{cases} \dfrac{k_l^t}{r^{\tau}} (p_l - p_t)^T (p_l - p_t) ? d_l^t < r^{\tau} \\ k_l^t \left\| p_l - p_t \right\|^T \quad , d_l^t \ge r^{\tau}. \end{cases} \tag{8}$$

From (7) and (8), the corresponding forces are generated as:

$$F_l^t = \begin{cases} -\dfrac{k_l^t}{r^{\tau}} d_l^t ? \ d_l^t < r^{\tau} \\ -k_l^t, \quad d_l^t \ {}^3 r^{\tau}. \end{cases} \tag{9}$$

The positive constants k_l^t, r^{τ} are used to regulate the fast approach to the target position, $d_l^t = \left\| p_l - p_t \right\|$ is the Euclidean distance. The sketch of these forces is depicted in Fig. 2.

The second component f_l^o , which is the total of repulsive forces of the obstacles, is created around the

obstacles to drive the leader to avoid the obstacles, see [1], [4]. This component is built as:

$$f_l^o = \sum_{o \in N_l^\beta(t)} F_l^o n_l^o - \sum_{o \in N_l^\beta(t)} k_l^{vo}\left(v_l - v_o\right) \quad (10)$$

where the set of β neighborhood of the leader at time t is $N_l^\beta(t)$. The obstacles o ($o \in N_l^\beta$(t)), which the leader must avoid, are defined as:

$$\left\{o \in N_l^\beta(t)\right\} = \left\{o, d_i^o \le r^\beta, o = 1,..M, o \ne i, o \ne l\right\} \quad (11)$$

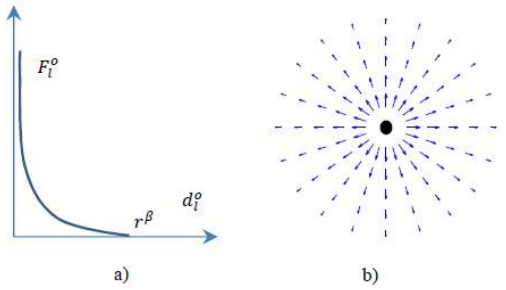

Figure 3. The repulsive force F_l^0(a) and vector field $F_l^0 n_l^o$ around the obstacle (b).

Here $r^\beta > 0$ is an obstacle detecting range and $\|q_o - q_l\| = d_l^o$ is the Euclidean distance. F_l^o, which depicted in Fig. 3, is the effect of the obstacle o ($o \in N_l^\beta$(t)) on the leader (see). It is designed as:

$$F_l^o = \begin{cases} k_l^o\left(\dfrac{r^\beta + k_l^\delta}{d_l^o + k_l^\delta} - 1\right)\dfrac{\left(r^\beta + k_l^\delta\right)}{\left(d_l^o + k_l^\delta\right)^2}, & 0 < d_l^o \le r^\beta \\ 0, & otherwise. \end{cases} \quad (12)$$

Similar to vector n_l^t, vector n_l^o is defined as $n_l^o = \dfrac{\left(p_l - p_o\right)}{\|p_l - p_o\|}$ and v_o is the velocity of the obstacle. The positive constants $(k_l^o, k_l^\delta, k_l^{vo})$ are applied to control the fast obstacles avoidance.

Finally, the control law for the leader is

$$\begin{aligned} u_l &= F_l^t n_l^t - k_l^{vt}\left(v_l - v_t\right) \\ &+ \sum_{o \in N_l^\beta(t)} F_l^o n_l^o - \sum_{o \in N_l^\beta(t)} k_l^{vo}\left(v_l - v_o\right). \end{aligned} \quad (13)$$

B. Control Algorithm for Each Member-Robot

The movement of each robot i is controlled by the sum force that consists of three components as follows:

$$u_i = f_i^j + f_i^o + f_i^l \quad (14)$$

The first component f_i^j of (14), which is used to control the connection of the robot i and its neighbors, consists of the attractive and repulsive forces between them. This total control force for the member-robot i is built as:

$$f_i^j = \sum_{j \in N_i^\alpha(t)} F_i^j n_i^j - \sum_{j \in N_i^\alpha(t)} k_i^{vj}\left(v_i - v_j\right) \quad (15)$$

where $n_i^j = \dfrac{\left(p_i - p_j\right)}{\|p_i - p_j\|}$ is a unit vector along the line connection p_i *to* p_j and k_i^{vj} is the positive amplification coefficient.

Because the communication of robots is only allowed to happen in the set of α neighborhood at time t, $N_i^\alpha(t)$ in (2), the potential field ($F_i^j n_i^j$) is characterized by a potential function V_i^j, which is calculated as follows:

$$V_i^j = \begin{cases} \dfrac{1}{2}k_i^{j1}\left(\dfrac{r_0^\alpha + k_i^{j2}}{d_i^j + k_i^{j2}} - 1\right)^2, & 0 < d_i^j < r_0^\alpha \\ k_i^{j3}\left(d_i^j - r_0^\alpha\right)^2, & r_0^\alpha < d_i^j \le r^\alpha \\ 0, & otherwise. \end{cases} \quad (16)$$

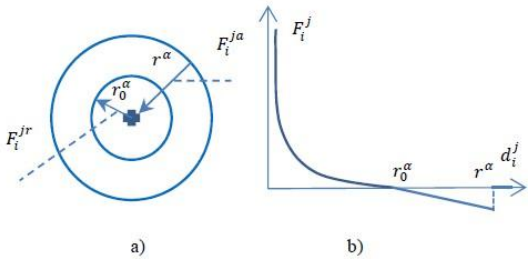

Figure 4. The radius of neighborhood circle (a) and the amplitude of the force of robot j acts on robot i (b).

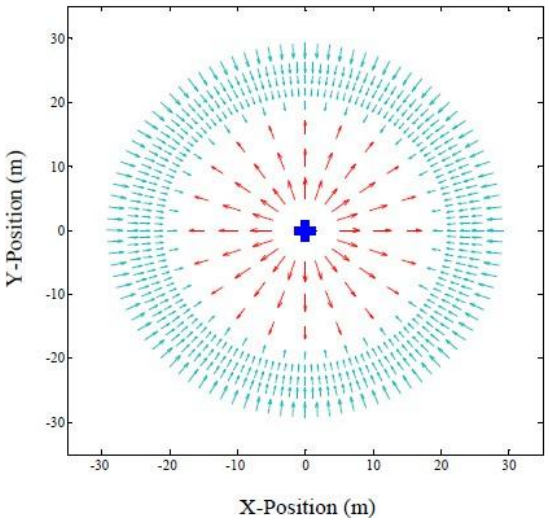

Figure 5. The attractive/repulsive potential field $F_i^j n_i^j$ around the robot j ($P_j = [0, 0]^T$) acts on robot i.

Taking the negative gradient of this V_i^j, we obtain a vector field $F_i^j n_i^j$ that is depicted in Fig. 5 as:

$$F_i^j n_i^j = -\nabla V_i^j \quad (17)$$

The force F_i^j describes the effect of the robot j $(j \in N_i^\alpha(t))$ on the robot i (see Fig. 4), which consists of the attractive force F_i^{ja} and the repulsive force F_i^{jr} (show in Fig. 4). From (17), this force is calculated as:

$$F_i^j = \begin{cases} k_i^{j1}\left(\dfrac{r_0^\alpha + k_i^{j2}}{d_i^j + k_i^{j2}} - 1\right)\dfrac{\left(r_0^\alpha + k_i^{j2}\right)}{\left(d_i^j + k_i^{j2}\right)^2}, 0 < d_i^j < r_0^\alpha \\ -2k_i^{j3}\left(d_i^j - r_0^\alpha\right) \quad , r_0^\alpha < d_i^j \le r^\alpha \\ 0 \quad , otherwise, \end{cases} \tag{18}$$

where d_i^j is the Euclidean distance in (2) and the positive constants ($k_i^{j1}, k_i^{j2}, k_i^{j3}$) are the regulate factors used to regulate the fast collisions, and the stability in the set of the α neighborhood of the robot i.

The interaction range (radius of neighborhood circle, show in Fig. 4, $r_0^\alpha, r^\alpha > 0$) describes the influence of the force F_i^j on the robot i. When $0 < d_i^j < r_0^\alpha$ then robot I and j repel each other to avoid the collisions between them. Otherwise, when $r_0^\alpha < d_i^j \le r^\alpha$ then they attract each other to approach the stable combination at the equilibrium position $(d_i^j = r_0^\alpha)$ in the set of α neighborhood of robot i. When $d_i^j > r^\alpha$ there is no interaction between these members.

The second component f_i^o of (14), which is the total repulsive force of the obstacles in the set of the β neighborhood of robot i $N_i^\beta(t)$, in (19), drives the robot I to avoid the obstacles.

$$\left\{o \in N_l^\beta(t)\right\} = \left\{o, d_i^j \le r^\beta, o = 1,..M, o \ne i, o \ne l\right\} \tag{19}$$

Similar to the f_l^o in (10), the force f_i^o is defined as:

$$f_i^o = \sum_{o \in N_i^\beta(t)} F_i^o n_i^o + \sum_{o \in N_i^\beta(t)} k_i^{vo}\left(v_o - v_i\right) \tag{20}$$

Here $n_i^o = \dfrac{\left(p_i - p_o\right)}{\left\|p_i - p_o\right\|}$ and $\left(v_i - v_o\right)$ are a unit vector and the relative velocity vector between robot i and obstacles respectively. The force F_i^o , which is an effect of the obstacles o $(o \in N_i^\beta(t))$ on the robot i, is computed as:

$$F_i^o = \begin{cases} k_l^o\left(\dfrac{\left(r^\beta + k_l^\delta\right)}{\left(d_i^o + k_l^\delta\right)} - 1\right)\dfrac{\left(r^\beta + k_l^\delta\right)}{\left(d_i^o + k_l^\delta\right)^2}, 0 < d_i^o < r^\beta \\ 0 \quad , d_i^o \ge r^\beta. \end{cases} \tag{21}$$

The positive constants $(k_l^o, k_l^\delta, k_i^{vo})$ are applied as the constants in (12) to regulate the fast obstacle avoidance for the robot i and $d_i^o = \left\|q_i - q_o\right\|$ is the Euclidean distance.

The third component f_i^l of (14) is the control force of the robot-leader to drive the trajectory of the robot i to follow it and to avoid the collision between them. It is described as:

$$f_i^l = F_i^l n_i^l + k_i^{vl}\left(v_l - v_i\right). \tag{22}$$

where, $n_i^l = \dfrac{\left(p_i - p_l\right)}{\left\|p_i - p_l\right\|}$ and $\left(v_i - v_l\right)$ are a unit vector along p_i *to* p_l and the relative velocity among them respectively. The force F_i^l is described as:

$$F_i^l = \begin{cases} k_i^{l1}\left(\dfrac{\left(r_0^\alpha + k_i^{l2}\right)}{\left(d_i^l + k_i^{l2}\right)} - 1\right)\dfrac{\left(r_0^\alpha + k_i^{l2}\right)}{\left(d_i^l + k_i^{l2}\right)^2}, 0 < d_i^l < r_0^\alpha \\ -2k_i^{l3}\left(d_i^l - r_0^\alpha\right) \quad , r_0^\alpha < d_i^l < r^\alpha \\ -k_i^{l4} \quad , d_i^l \ge r^\alpha. \end{cases} \tag{23}$$

where, $d_i^l = \left\|q_i - q_l\right\|$ is the Euclidean distance and $(k_i^{l1}, k_i^{l2}, k_i^{l3}, k_i^{l4})$ are the positive factors.

Finally, the control law for the robot i is

$$\begin{aligned} u_i = & \sum_{j \in N_i^\alpha(t)} F_i^j n_i^j - \sum_{j \in N_i^\alpha(t)} k_i^{vj}\left(v_i - v_j\right) \\ & + \sum_{o \in N_i^\beta(t)} F_i^o n_i^o - \sum_{o \in N_i^\beta(t)} k_i^{vo}\left(v_i - v_o\right) \\ & + F_i^l n_i^l - k_i^{vl}\left(v_i - v_l\right). \end{aligned} \tag{24}$$

IV. Stability Analysis

Based on the ideal for the stability and robustness of the desired swarm presented in part II, which is expressed by the constant distances between the robots in the neighborhood of them. In order to analyze the stability of the swarm we analyze the stability of a robot i $(\mathrm{i} = 1...\mathrm{N})$ with its neighbors. Consider the relative positions of the robot i with others in the $N_i^\alpha(t)$ (2), which is described by the dynamic model as follows:

$$\begin{cases} \dot{x}_1 = x_2 \\ \dot{x}_2 = u. \end{cases} \tag{25}$$

where, $x_1 = p_i - p_j, x_2 = v_i - v_j$ are the relative position and velocity of the robot i and j. Consider the system (25) without the effect of the leader in the free space, we have:

$$\dot{x}_2 = \dot{v}_i - \dot{v}_j = u_i - u_j \tag{26}$$

Substituting equation (14) and (24) into (26), we obtain as follows:

$$\begin{aligned} \dot{x}_2 &= 2\sum_{j \in N_i^\alpha(t)} F_i^j n_i^j - 2\sum_{j \in N_i^\alpha(t)} k_i^{vj}\left(v_i - v_j\right) \\ &= -2\sum_{j \in N_i^\alpha(t)} \left(\nabla \mathrm{V}_i^j\right)^T - 2\sum_{j \in N_i^\alpha(t)} k_i^{vj} x_2. \end{aligned} \tag{27}$$

To analyze the stability of model (25) at the equilibrium point, at which the distance between the member-robot i and its neighbors j achieves a desired value $\|q_i - q_j\| = r_0^{\alpha}$ (see in Fig. 4), the Lyapunov function can be selected as in [8], [9]:

$$V = 2\sum_{j\in N_i^{\alpha}(t)} V_i^j + \frac{1}{2}x_2^T x_2 \tag{28}$$

Taking the time derivative of (28) along the trajectories of the system (25), we get:

$$\begin{aligned}\dot{V}(t) &= 2\sum_{j\in N_i^{\alpha}(t)} (\nabla V_i^j)^T \dot{x}_1 + x_2^T \dot{x}_2 \\ &= x_2^T\left(2\sum_{j\in N_i^{\alpha}(t)} (\nabla V_i^j) + \dot{x}_2\right)\end{aligned} \tag{29}$$

If substitute (25) for $\dot{x}_2$ into (27), the time derivative of the chosen Lyapunov function V will be as:

$$\dot{V}(t) = -2\sum_{j\in N_i^{\alpha}(t)} k_i^{vj} x_2^T x_2 \le 0 \tag{30}$$

This result guarantees the stability of the swarm at the equilibrium position.

V. UAV Model and Control

The dynamic model of the UAV in the state-space is presented in this section as depicted in Fig. 6.

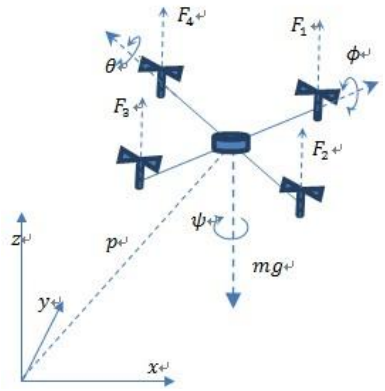

Figure 6. Structure of the UAV

The generalized coordinates for this model are the following:

$$\xi_i = (\mathrm{x}_i, \mathrm{y}_i, \mathrm{z}_i\ \phi_i, \theta_i, \psi_i)^T \in \mathrm{R}^6 \tag{31}$$

where $\eta_i = (\phi_i, \theta_i, \psi_i)^T \in R^3$ denotes the Euler angles (roll, pitch and yaw respectively) which describes the rotational movement of the UAV, and $p_i = (\mathrm{x}_i, \mathrm{y}_i, \mathrm{z}_i)^T \in R^3$ is the position of the center of mass of the UAV in the three-dimensional space, which describes the translational motion of the UAV.

In [10], Samir Bouabdallah and Roland Siegwart proposed the full dynamic model for the UAV in the state space and a backstepping controller. The model is given by

$$\begin{cases} \ddot{x}_i = \dfrac{1}{m}(\cos\phi_i \sin\theta_i \cos\psi_i + \sin\phi_i \sin\psi_i)U_1 \\ \ddot{y}_i = \dfrac{1}{m}(\cos\phi_i \sin\theta_i \sin\psi_i - \sin\phi_i \cos\psi_i)U_1 \\ \ddot{z}_i = \dfrac{1}{m}(\cos\phi_i \cos\theta_i)U_1 - g, \end{cases} \tag{32}$$

$$\begin{cases} \ddot{\phi}_i = \dot{\theta}_i\dot{\psi}_i(\dfrac{I_y - I_z}{I_x}) + \dot{\theta}\omega\dfrac{J_x}{I_x} + \dfrac{l}{I_x}U_2 \\ \ddot{\theta}_i = \dot{\theta}_i\dot{\psi}_i(\dfrac{I_z - I_x}{I_y}) + \dot{\phi}_i\omega\dfrac{J_x}{I_y} + \dfrac{l}{I_y}U_3 \\ \ddot{\psi}_i = \dot{\theta}_i\dot{\phi}_i(\dfrac{I_x - I_y}{I_z}) + \dfrac{1}{I_z}U_4, \end{cases} \tag{33}$$

where the parameters m, g, l, $I_{x,y,z}$, J are the mass of UAV, the gravitational constant, the lever of the arm length of UAV, the body moment of inertia around the x, y, z axis and rotor inertia, respectively. The four rotors rotate at four angular velocities ω_e $(\mathrm{e}=1...4)$ which produce four forces F_e to direct the UAV upward. The control inputs of the system $(U_1, U_x, U_y, U_2, U_3, U_4)$ and the control parameter (ω) are computed as follows:

$$\begin{cases} \mathrm{U}_x = \cos\phi_i \sin\theta_i \cos\psi_i + \sin\phi_i \sin\psi_i \\ \mathrm{U}_y = \cos\phi_i \sin\theta_i \sin\psi_i - \sin\phi_i \cos\psi_i \end{cases} \tag{34}$$

$$\begin{cases} \mathrm{U}_1 = b(\omega_1^2 + \omega_2^2 + \omega_3^2 + \omega_4^2) \\ \mathrm{U}_2 = b(\omega_4^2 - \omega_2^2) \\ \mathrm{U}_3 = b(\omega_3^2 - \omega_1^2) \\ \mathrm{U}_4 = db(-\omega_1^2 + \omega_2^2 - \omega_3^2 + \omega_4^2) \\ \omega = \omega_2 + \omega_4 - \omega_1 - \omega_3, \end{cases} \tag{35}$$

here b is thrust factor and d is positive constant.

Backstepping, that is one of the effective nonlinear control methods, can be applied to design the controllers $U = (U_1, U_x, U_y, U_2, U_3, U_4)$ of the system.

Firstly, control input U_1 is used to control the altitude of the UAV as:

$$U_1 = \frac{m}{\cos\phi_i \cos\theta_i}\left[(1+\lambda_1\lambda_2)(\mathrm{z}_d - \mathrm{z}_i) - (\lambda_1 + \lambda_2)\dot{\mathrm{z}}_i + g\right]. \tag{36}$$

Secondly, control inputs U_x, U_y are used to control the positions x and y of the UAV as:

$$U_x = \frac{m}{U_1}\left[(1+\lambda_3\lambda_4)(\mathrm{x}_d - x_i) - (\lambda_3 + \lambda_4)\dot{\mathrm{x}}_i\right] \tag{37}$$

$$U_y = \frac{m}{U_1}\left[(1+\lambda_5\lambda_6)(\mathrm{y}_d - y_i) - (\lambda_5 + \lambda_6)\dot{\mathrm{y}}_i\right] \tag{38}$$

From (37) and (38), the control inputs ϕ_d (the desired roll) and θ_d (the desired pitch) of the attitude control loop are computed as follows:

$$\phi_d = \arcsin(\mathrm{U}_x \sin\psi_d - \mathrm{U}_y \cos\psi_d) \quad (39)$$

$$\theta_d = \arcsin(\frac{\mathrm{U}_x \cos\psi_d + \mathrm{U}_y \sin\psi_d}{\cos\phi}) \quad (40)$$

Thirdly, control inputs U_2, U_3, U_4 are applied to control the attitude of the system as:

$$U_2 = \frac{1}{b_1}\left[(1+\lambda_7\lambda_8)(\phi_d - \phi_i) - (\lambda_7+\lambda_8)\dot{\phi}_i - \dot{\theta}_i\dot{\psi}_i a_1 - \dot{\theta}_i \omega a_2\right], (41)$$

$$U_3 = \frac{1}{b_2}\left[(1+\lambda_9\lambda_{10})(\theta_d - \theta_i) - (\lambda_9+\lambda_{10})\dot{\theta}_i - \dot{\phi}_i\dot{\psi}_i a_3 - \dot{\phi}_i \omega a_4\right], \quad (42)$$

$$U_4 = \frac{1}{b_3}\left[(1+\lambda_{11}\lambda_{12})(\psi_d - \psi_i) - (\lambda_{11}+\lambda_{12})\dot{\psi}_i - \dot{\phi}_i\dot{\theta}_i a_5\right], \quad (43)$$

where $a_1 = \frac{I_y - I_z}{I_x}, a_2 = \frac{J}{I_x}, a_3 = \frac{I_z - I_x}{I_y}, b_1 = \frac{l}{I_x}, b_2 = \frac{l}{I_y}, \mathrm{b}_3 = \frac{1}{I_z}$, $a_5 = \frac{I_x - I_y}{I_z}, a_4 = \frac{J}{I_y}, b_1 = \frac{l}{I_x}, b_2 = \frac{l}{I_y}$,and $\lambda_\zeta (\zeta = 1,..12)$ are the positive factors. The parameter z_d is the desired altitude of the swarm, which is chosen as the altitude of the target, and the altitude tracking error is $z_\zeta = (z_d - z_i)$. For a detailed presentation of this backstepping controller see [10].

Based on these controllers combined with the designed formation controllers in section III, the control architecture for each UAV in the swarm is proposed in Fig. 7.

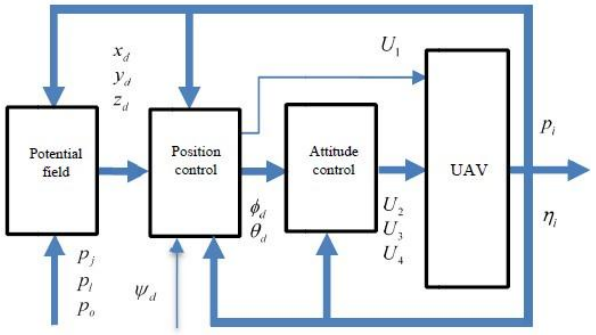

Figure 7. The control architecture of a UAV

VI. Simulation Results

This section presents the simulation results for the formation control algorithm of the UAVs. For the simulations, we assume that the initial velocities of the robots are set to zero and obstacles of the environment are stationary and their positions have been determined. The general parameters for simulation are listed in Table I.

First of all we test the control algorithm for the robot-leader tracking the target position.

Case 1: Consider the target does not move, that is, as a point in the free space. For the simulation it has the position $p_l = (30, 20, 10)^T$, and the initial position of the leader is $p_l = (0, 0, 0)^T$.

TABLE I. Parameter Values

Type	Parameter	Value
Potential field	r_0^α	20 m
	r^α	30 m
	r^β	30 m
	r^r	50 m
	k_l^t	0,5
	$k_l^{vt}=k_i^{vj}$	0,8
	k_i^{vl}	0,6
	$k_l^{vo}=k_i^{vo}$	0,6
	k_l^o	100
	k_l^δ	5
	$k_i^{j1}=k_i^{l1}$	50
	$k_i^{j2}=k_i^{l2}$	1,2
	$k_i^{j3}=k_i^{l3}$	0,06
	k_i^{l4}	0,01
UAV model	m	1 kg
	l	0,3 m
	I_x	$5{,}15.10^{-3}$ kg.m^2
	I_y	$5{,}15.10^{-3}$ kg.m^2
	I_z	$9{,}31.10^{-3}$ kg.m^2
	J	$3{,}26.10^{-5}$ kg.m^2
	b	$2{,}59.10^{-6}$kg.m
	d	1
	z_d	10 m
	g	9,81 m/s^2

Case 2: Consider the target moves along the trajectory $p_l = (0.3t + 11, -0.2t + 13)^T$ and the initial position of the leader is $p_l = [0, 0]^T$.

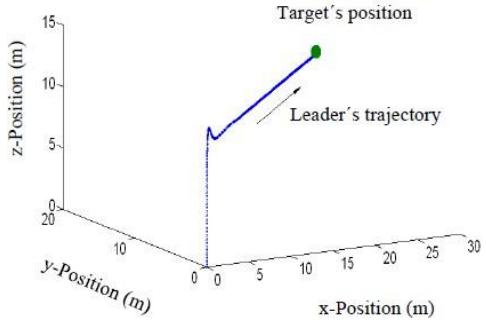

Figure 8. The trajectory of the leader reaches the position of the target in three-dimensional space.

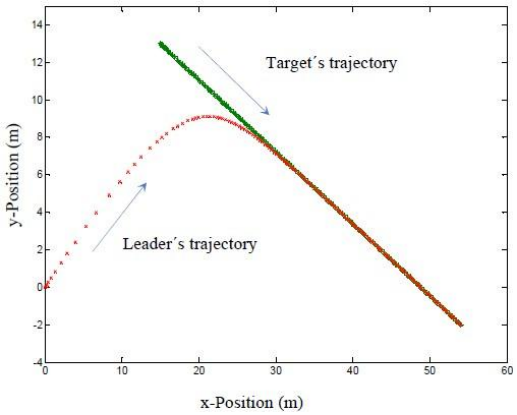

Figure 9. The trajectory of the leader tracks the moving target without obstacles of the environment.

The simulation result in Fig. 8 shows that while reaching to the position of the target the altitude of the

leader is always kept stable by the controller (36). The trajectory of the leader is always to reach the trajectory of the target, which is shown in the Fig. 9.

Second, the algorithm of the formation control, the leader-following motion of the swarm, the obstacles avoidance, the collision avoidance between robots in the swarm and the stability of the swarm while moving are verified by simulation.

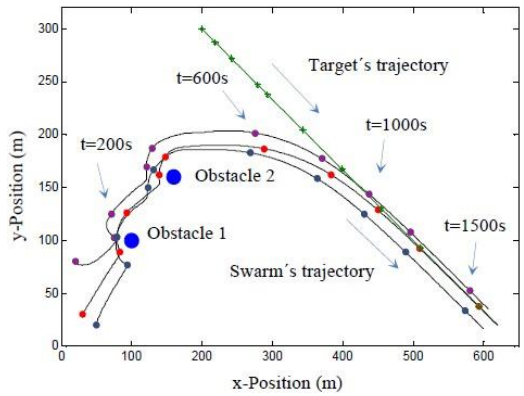

Figure 10. Swarm of three robots tracks a moving target in obstacle environment, the leader is red.

The simulation case for the swarm of three robots (shown in Fig. 10, Fig. 11), the initial position of the robots, obstacles and the target are as follows:

$$\mathrm{p}_1 = (20,80)^T, \mathrm{p}_2 = (50,20)^T, \mathrm{p}_l = (30,40)^T, \mathrm{p}_{o1} = (100,100)^T$$
$$\mathrm{p}_{o2} = (160,160)^T, \mathrm{p}_t = (0.3t + 200, -0.2t + 300)^T$$

Simulation results depicted in Fig. 10 and Fig. 11 show that the organization of a swarm of three robots is influenced by obstacles of the environment and target's trajectory while it tracks the moving target. At t=100s and t=150s the swarm avoided obstacles effectively, but the formation is broken while avoiding these obstacles (distances between robots in the swarm always changes from t=0 to t=600s, see in Fig. 11). Since time t=600s the stability of the swarm is set and maintained (distances between robot are constant, see in Fig. 11), swarm's trajectory always reached the target's trajectory.

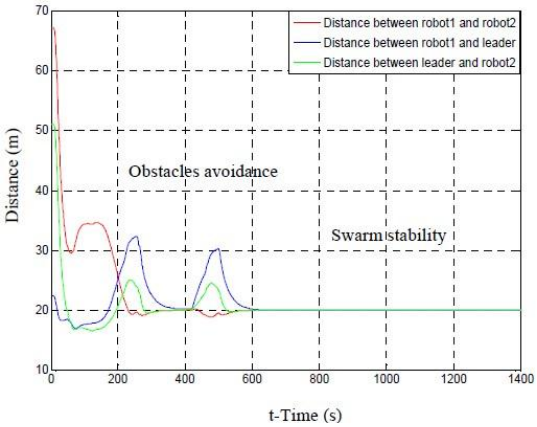

Figure 11. Distance between robots in the swarm.

The simulation case for the swarm of seven robots (shown in Fig. 12), the initial position of the robots, obstacles and the target are as follows:

$$\mathrm{p}_l = (30,150)^T, \mathrm{p}_1 = (10,10)^T, \mathrm{p}_2 = (20,80)^T, \mathrm{p}_3 = (10,40)^T,$$
$$\mathrm{p}_4 = (10,250)^T, \mathrm{p}_5 = (20,300)^T, \mathrm{p}_6 = (20,280)^T, \mathrm{p}_7 = (30,150)^T$$
$$\mathrm{p}_o = (130,250)^T, \mathrm{p}_t = (0.3t + 150, -0.2t + 350)^T.$$

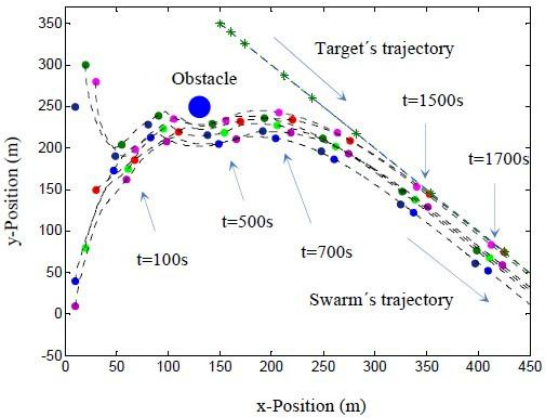

Figure 12. Swarm of seven robots avoids obstacle to track a moving target, the leader is red.

Fig. 12 shows that at initial time t=0 there are no communications between members in swarm, but after time t=100s, under the effect of the attractive force field of the leader these members have found their swarm quickly. The organization of the swarm starts set stable at t=200s. Obstacle avoidance is achieved successfully at t=500s. However, the stability and robustness of swarm is broken while avoiding this obstacle and then it is reset at t=700s and always maintained while the swarm tracks a moving target.

VII. Conclusion

This paper presents an approach for formation control of a UAVs swarm to track a moving target under the drive of a robot-leader based on the potential field method combined with a state feedback controller. The proposed formation control algorithms are verified by the simulations. The simulation results have shown that this is one of the control methods that can be applied to formation control of the flying multi-robots. The main advantages of this method are that the member-robots can find their swarm easily and quickly by the attractive field of the leader and in fast path searching to the target's position. However, the disadvantage of this method is that the function of the swarm depends always on the leader. Hence, the success of this method depends on further developments such as the intelligent swarm-finding of the member-robots without the drive of the leader in formation control to track a moving target. Furthermore, the algorithmic build to determine the position and velocity of the moving obstacles, and the adaptive and optimal formation control to avoid these obstacles will be the interesting and needful topics for our future research.

Acknowledgment

This research work is supported by the Vietnamese Government, MOET (Ministry of Education and Training) program.

REFERENCES

[1] F. E. Schneider and D. Wildermuth, "A potential field based approach to multi robot formation navigation," in *Proc. IEEE Intl. Conf. on Robotics, Intelligent System and Signal Processing*, October 2003, pp. 680-685.

[2] P. Shi and Y. W. Zhao, "An efficient path planning algorithm for mobile robot using improved potential field," in *Proc. IEEE Intl. Conf. on Robotics and Biomimetics*, December 2003, pp. 1704-1708.

[3] S. S. Ge and Y. J. Cui, "New potential functions for mobile robot path planning," *IEEE Trans. on Robotics and Automation*, vol. 16, no. 5, pp. 615-620, October 2000.

[4] K. H. Kowdiki, R. K. Barai, and S. Bhattacharya, "Leader-follower formation control using artificial potential functions: A kinematic approach," *IEEE Intl. Conf. on Advances in Engineering, Science and Management*, pp. 500-505, March 2012.

[5] N. E. Leonard and E. Fiorelli, "Virtual leader, artificial potential and coordinated control of groups," in *Proc. 40th IEEE Conf. on Decision and Control*, December 2001, pp. 2968-2973.

[6] J. Wang, X. B. Wu, and Z. L. Xu, "Decentralized formation control and obstacles avoidance based on potential field method," in *Proc. Fifth Intl. Conf. on Machine Learning and Cybernetics*, August 2006, pp. 803-808.

[7] H. M. La and W. H. Sheng, "Flocking control of multiple agents in noisy environments," *IEEE Intl. Conf. on Robotics and Automation*, May 2010, pp. 4964-4969.

[8] S. Bandyopadhyay, C. M. Saaj, and B. Bandyopadhyay, "Stability analysis of small satellite formation flying and reconfiguration missions in deep space," in *Proc. 12th IEEE Workshop on Variable Structure System, VSS'12*, January 2012, pp. 285-290.

[9] R. A. Freeman and P. V. Kokotović, *Robust Nonlinear Control Design: State-Space and Lyapunov Techniques*, Birkhäuser, 1996.

[10] S. Bouabdallah and R. Siegwart, "Backstepping control and sliding-mode techniques applied to an indoor micro quadrotor," in *Proc. IEEE Intl. Conf. on Robotics and Automation*, April 2005, pp. 2259-2264.

[11] A. Abdessameud and A. Tayebi, "Formation control of VTOL-UAVs," in *Proc. Joint 48th IEEE Conf. on Decision and Control and 28th Chinese Control Conference*, December 2009, pp. 3454-3459.

[12] L. G. Delgado, A. Dzul, V. Santibánez, and M. Llama, "Quad-rotor formation control as an interconnected system," in *Proc. Preprints of the 18th IFAC World Congress*, August 2011, pp. 13582-13587.

AnhDuc Dang was born in Thai Nguyen, Vietnam in 1977. He received his M.Sc. degree in Control Engineering from Thai Nguyen University of Technology in 2005. Now he is working toward the Ph.D. degree at the University of the Federal Armed Forces Hamburg, Germany.His research interests include nonlinear control, multi-agent system, path planning, Formation control, Potential field, Aircraft control.

Joachim Horn received the Dipl.-Ing. degree in electrical engineering from the University of Karlsruhe, Germany, in 1989 and the Dr.-Ing.degree in electrical engineering from the Technical University of Munich, Germany, in 1996.He was with the Department of Automatic Control Engineering, Technical University of Munich, from 1990 to 1995 and with Siemens Corporate Technology, Munich, from 1996 to 2004. Since 2004, he is a Professor for Automatic Control Engineering in the Department of Electrical Engineering, Helmut Schmidt University / University of the Federal Armed Forces Hamburg. His research interests include robotics, control of fuel cell systems, and nonlinear filtering.